CHEMISTRY
A EUROPEAN JOURNAL

DOI: 10.1002/chem.200801505

Chirality in the Absence of Rigid Stereogenic Elements: The Design of Configurationally Stable C_3-Symmetric Propellers

Tiziana Benincori,[a] Andrea Marchesi,[b] Tullio Pilati,[c] Alessandro Ponti,*[c] Simona Rizzo,[c] and Francesco Sannicolò*[c, d]

Dedicated to Sofia Giovanna

Abstract: Residual stereoisomerism is a form of stereoisomerism scarcely considered so far for applicative purposes, though extremely interesting, since the production of stereoisomers does not involve classical rigid stereogenic elements. In three-bladed propeller-shaped molecules, a preferred stereomerization mechanism, related to the correlated rotation of the rings, allows the free interconversion of stereoisomers inside separated sets (the residual stereoisomers) that can interconvert through higher energy pathways. In light of possible future applications as chiral ligands for transition metals in stereoselective processes, some C_3-symmetric phosphorus-centered propellers, which could exist as residual enantiomers, are synthesized and the possibility of resolving their racemates into residual antipodes is explored. While the tris(aryl)methanes are configurationally stable at room temperature, only selected tris(aryl)phosphane oxides display a configurational stability high enough to allow resolution by HPLC on a chiral stationary phase (CSP HPLC) at a semipreparative level at room temperature. Stability was evaluated through different techniques (circular dichroism (CD) signal decay, dynamic CSP HPLC (CSP DHPLC), dynamic NMR analysis (DNMR)) and the results compared and discussed. Phosphanes were found much less stable than the corresponding phosphane oxides, for which preliminary calculations suggest that the three-ring-flip enantiomerization mechanism (M_0) would be easier than phosphorus pyramidal inversion. The parameters affecting the configurational stability of the residual enantiomers of C_3-symmetric propellers are discussed.

Keywords: chirality · circular dichroism · NMR spectroscopy · phosphane oxides · phosphanes · residual enantiomers

Introduction

The metal complexes of tris(aryl)phosphanes bearing three identical aryl rings are amongst the most popular mediators in homogeneous catalysis.[1] It is common knowledge that they are propeller-shaped chiral compounds, but chemists have always accepted their configurational instability as an unavoidable event due to the very easy helix reversal, and rarely contemplated the possibility of taking profit of their inherent chirality.

Attempts to investigate the facial recognition ability of propeller helicity generally follows the strategy of introducing chiral substituents on the aryl rings of tris(aryl)phosphanes in the hope that they could stabilize a preferred helical configuration.[2] It is, however, difficult to discriminate the effects attributable to the helix from those referable to the substituents. Some chiral configurationally stable metal complexes of a tris{3-[1-(diphenylphosphino)-2-

[a] Prof. T. Benincori
Dipartimento di Scienze Chimiche ed Ambientali
Università dell'Insubria
via Valleggio 11, 22100 Como (Italy)

[b] Dr. A. Marchesi
Laboratori Alchemia s.r.l.
via S. Faustino 68, 20134 Milano (Italy)

[c] Dr. T. Pilati, Dr. A. Ponti, Dr. S. Rizzo, Prof. F. Sannicolò
Istituto di Scienze e Tecnologie Molecolari
Consiglio Nazionale delle Ricerche
via Golgi 19, 20133 Milano (Italy)
Fax: (+39) 0250314300
E-mail: alessandro.ponti@istm.cnr.it

[d] Prof. F. Sannicolò
Dipartimento di Chimica Organica e Industriale
C.I.MA.I.NA., Università di Milano
via Venezian 21, 20133 Milano (Italy)
Fax: (+39) 0250314139
E-mail: francesco.sannicolo@unimi.it

methyl]benzimidazolyl}methane were recently described and applied in a carbon-carbon bond-forming reaction.[3]

We considered that, at least in principle, chiral and configurationally stable tris(aryl)phosphanes could be obtained as residual enantiomers as long as their structural architecture could satisfy the conditions required for the existence of residual stereoisomerism, a phenomenon discovered by Prof. K. Mislow in the 1970s.[4] Residual stereoisomers "result whenever closed subsets of appropriately substituted interconverting isomers are generated from a full set under the operation of a given stereomerization" mechanism. The residual stereoisomers isolated so far are produced by two similar phenomena working in very different molecular architectures: the dynamic gearing operating in the case of bis(trypticyl)methanes[5] and ethers[6] and the correlated rotation of the rings in the case of three-bladed molecular propellers, such as tris(aryl)methanes[7] and tris(aryl)amines,[8] in which three aryl rings devoid of local C_2 axes (the blades) radiate from a central carbon or nitrogen atom (the hub).[9] The first classical example belonging to the latter class of molecules is the maximally labeled (three differently substituted aromatic rings) compound **1**, for which a full set of 32 chiral stereoisomers are predicted. They are generated by

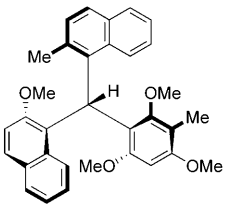

1

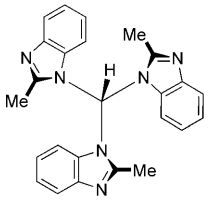

2

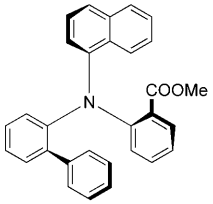

3

the stereocenter lying on the hub, by the helicity, and by the three different simple rotors describing the conformations resulting from the rotation of the aryl rings around the C_{sp^3}–$C_{aromatic}$ bonds. In other words, ring rotation corresponds to ring edge interchange with respect to the reference plane (the plane defined by the three neighboring sp^2 carbon atoms bound to the central sp^3 carbon atom). It has been firmly established that in these systems "the motion of the rings is coupled"[7] and that any isomerization process involves helicity reversal.[4c]

There are four theoretically possible stereomerization mechanisms M_n ($n=0$, 1, 2, 3), which are characterized by the number n of rings undergoing edge interchange. The rings not involved in edge interchanging are said to flip, that is they pass through the plane containing the C_{sp^3}–$C_{aromatic}$ bond and perpendicular to the reference plane. The M_1 mode, which involves one edge interchange and two ring-flips, is, without known exceptions, the threshold stereomerization mechanism. This mechanism does not allow free interconversion within the full set of stereoisomers displaying the same configuration at the stereogenic carbon, but only within closed subsets, which constitute the residual diastereoisomers. The absolute preference for the M_1 mode had was demonstrated recently by ^{1}H NMR spectroscopy in the case of an unlabeled tris(mesytyl)phosphonium cation associated to chiral C_3-symmetric counterions.[10]

In the case of **1**, two residual racemic diastereoisomers were separated by crystallization. Each racemate is made up of two enantiomeric non-interconvertible (*R*,*S*) sets of eight diastereoisomers, rapidly interconverting at 87 °C by the M_1 mechanism with stereomerization barriers of about 10–15 kcal mol^{-1}. The interconversion of diastereomeric residual racemates started to be active at 122 °C, with a quite high barrier ($\Delta G^{\neq}=30.5$ kcal mol^{-1} at 122 °C) as demonstrated by ^{1}H dynamic NMR detected kinetics.

As two configurationally stable diastereomeric couples of enantiomers are observable in the case of propeller **1**, it is expected that a couple of configurationally stable enantiomers would be obtained by removing the stereogenicity of the carbon atom on the hub, simply by using at least two identical aryl rings connected to it. This was demonstrated eighteen years ago by the successful chromatographic resolution of the residual racemate of C_3-symmetric tris[1-(2-methyl)benzimidazolyl)]methane (**2**).[11] Also in this case the enantiomerization barrier was found to be considerable ($\Delta G^{\neq}=28.5$ kcal mol^{-1} at 70 °C).

The crucial role played by the nature of the atom located on the hub of the helix was clearly demonstrated by Mislow in the case of the maximally labeled tris(aryl)amine **3**.[8] Two achiral diastereomers are expected for this system, since fast nitrogen pyramidal inversion corresponds to a planar equilibrium geometry analogous to that shown by tris(aryl)boranes. The separation of the residual diastereoisomers was achieved by taking advantage of their different, easily distinguishable, crystalline forms. The configurational stability of the residual diastereoisomers was found to be much lower than that exhibited by the carbon-centered propellers ($\Delta G^{\neq}=17.7$ kcal mol^{-1} at −21 °C), probably due to the fact that the level of the dynamic gearing amongst the rings, which is responsible for the configurational stability of the residual stereoisomers, is strongly diminished when pyramidality is lost, and the aryl rings diverge in the transition state required for the nitrogen inversion process.

The present paper reports the results of the development of a work of which we have given only a short preliminary account in the case of tris[3-(2-alkyl)indolyl]phosphane oxides **4a**, **4e**, and **4f**.[12] The multi-targeted project was focused on:

1) Designing, on the basis of previous experiments and DFT calculations, phosphorus-centered propellers of the Ar_3P-X type (X = oxygen, lone pair), devoid of any rigid stereogenic element, which would be promising for generating stable residual enantiomers.
2) Synthesizing the compounds.
3) Structurally characterizing the new compounds, possibly by XRD analysis.
4) Resolving the residual racemates.

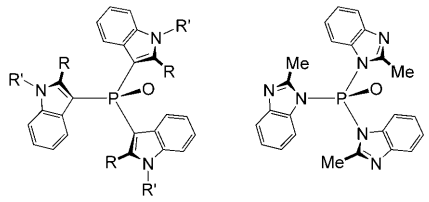

4 5

a	R = Me	R' = Me
b	R = CH_2D	R' = Me
c	R = CH_2OMe	R' = Me
d	R = Me	R' = Et
e	R = Et	R' = Me
f	R = *i*Pr	R' = Me
g	R = CH_2Br	R' = Me
h	^{2}R = Et, ^{1}R = H	R' = Me

5) Evaluating the enantiomerization barriers of the residual enantiomers by different techniques (circular dichroism (CD), CSP dynamic HPLC (CSP DHPLC), and ^{1}H NMR spectroscopy)
6) Discussing their dependence upon some specific structural features.

In particular, we planned to consider the effects produced on configurational stability by four structural parameters:

1) The hub–aryl bond length: the length of the P–$C_{aromatic}$ bond is much greater (1.78 Å) than that exhibited by the C_{sp^3}–$C_{aromatic}$ bond (1.54 Å) in **1** and, even more so, by the C_{sp^3}–$N_{aromatic}$ bond (1.45 Å) in **2**. Thus, the correlated rotation of the rings is expected to be less effective in phosphorus- than in carbon-centered propellers.
2) The aryl-hub-aryl angles characterizing the propeller: the wider the angles, the lower the engagement of the rings, and the lower the expected configurational stability.
3) The bulkiness of the substituents located in the *ortho* position on the aromatic rings: the bulkier the groups, the stronger the inter-ring dynamic gearing, and then the higher the configurational stability
4) The barrier for the pyramidal inversion of the phosphorus atom in tris(aryl)phosphanes: it is known to be higher than in tris(aryl)amines, but not so high to guarantee configurational stability at room temperature.[13]

We started the research by paying attention to the behavior of phosphane oxides, since we wanted to preliminarily check whether an efficient dynamic gearing could be achieved in non-inverting phosphorus-centered propellers. Furthermore, efficient methodologies are available for the resolution of racemic phosphane oxides, while the resolution of racemic phosphanes is more difficult (particularly at an analytical level) so that enantiopure phosphanes are generally prepared by reduction of the corresponding enantiopure phosphane oxides.[14]

We have chosen the 1,2-disubstituted-3-indolyl group as the aryl *ortho*-differentiated aromatic ring, since its synthetic versatility offers the possibility of acceding to an ample modular series of compounds **4**, in which the effects of the different size of the group located in the 2-position of the indole ring could give interesting information on the efficiency of the correlated ring rotation and, in turn, on the configurational stability of the residual enantiomers. In this light, we prepared phosphane oxides **4a**, **4e**, and **4f**, in which the correlated rotation of the ring should be progressively enhanced.

We also considered worth synthesizing the tris[1-(2-methyl)benzimidazolyl]phosphane oxide (**5**), which, unlike **2**, is a phosphorus-centered system with identical blades. It could give interesting quantitative information on the role of the atom located on the propeller axis, since it controls both the hub–blade distance and the pyramidality of the systems. In this light, in order to perform a direct comparison under identical experimental conditions, we prepared and reinvestigated known tris[1-(2-metyl)benzimidazolyl]methane (**2**).

Results and Discussion

Computational study of compound 4: We resorted to computational electronic structure methods to check a few points that we considered crucial for the successful development of the research project. Some results at the B3LYP/3-21G* level have already been published.[12] There we showed that the *Psss*/*Msss*[15] are the major isomers and that the M_0 enantiomerization barrier significantly depends on the size of substituent R to the extent that **4f** is configurationally stable enough to be resolved into residual enantiomers at room temperature, whereas **4a** is not. We extended the above investigation by performing both HF and DFT-B3LYP calculations using a much larger basis set (cc-pVDZ). The solvent effect has also been studied within the framework of the polarized continuum model (PCM).[16] The most significant energetic results are shown in Table 1.

We begin considering in vacuo results. Both HF and B3LYP results indicate that the *sss* isomers are the most stable and largely the major ones. The *ssa* conformers represent a few percent of the isomers, whereas the *aas* and the *aaa* diastereoisomers are virtually absent. Since **4a**, **4e**, and **4f** essentially comprise the *sss* and *ssa* stereoisomers, we calculated the activation barriers for the M_0 enantiomerization *Msss*→*Psss* and for the M_1 diastereomerization *Psss*→*Mssa* (or *Msss*→*Pssa*) processes. (The M_2 and M_3 stereomerization paths are virtually impossible, because of the huge steric hindrance produced when more than one indolyl moiety undergoes edge interchange.) In all cases the M_1 barrier is much lower than the M_0 barrier, so that the M_1 diastereomerization *within* each residual enantiomer is much faster than the M_0 interconversion *between* residual enantiomers. At room temperature (thermal energy $\approx$0.6 kcal mol^{-1}) the M_1 processes can be considered fast from the standpoint of configurational stability.[17] In contrast, the barriers for the M_0 processes are large enough at room temperature that the individual residual enantiomers

Table 1. Calculated energetics of tris[3-(1-methyl-2-R)indolyl]phosphane oxides **4a** (R = Me), **4e** (R = Et), and **4f** (R = *i*Pr).[a]

	$\Delta E(ssa-sss)$ [kcal mol^{-1}]	*P(sss):P(ssa)*	$\Delta E^{\neq}$ (M_0)[b] [kcal mol^{-1}]	$\Delta E^{\neq}$ (M_1)[c] [kcal mol^{-1}]
	2.7	*97.0:3.0*	*25.2*	*6.9*
4a	**2.6**	**96.6:3.4**	**19.9**	**7.0**
	1.2	72.4:27.6	19.9	4.0
	3.7	*99.4:0.6*	*26.0*	*10.6*
4e	**2.8**	**97.4:2.6**	**20.2**	**7.7**
	1.1	68.5:31.5	19.1	5.3
	4.1	*99.7:0.3*	*32.1*	*11.3*
4f	**3.1**	**98.4:1.6**	**24.6**	**8.0**
	1.3	75.1:24.9	23.6	5.9

[a] The energy difference between the two most stable *sss* and *ssa* isomers $\Delta E(ssa-sss)$ and the corresponding population ratio (*P*) ratio at room temperature are reported along with the activation energies for selected M_0 and M_1 isomerization processes. *Italic*: *HF/cc*-pVDZ, **Bold**: **B3LYP/cc-pVDZ**, Roman: PCM-B3LYP/cc-pVDZ. [b] For the *Msss* → *Psss* process. [c] For the *Psss*→*Mssa* or *Msss*→*Pssa* processes; for the reverse processes the $\Delta E(ssa-sss)$ energy difference should be subtracted from the reported value.

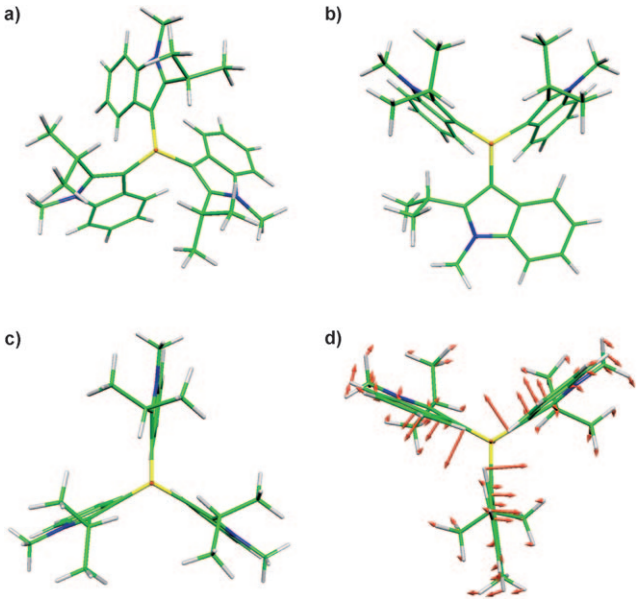

Figure 1. Selected B3LYP/cc-pVDZ optimised structures of tris[3-(1-methyl-2-isopropyl)indolyl]phosphane oxide (**4f**). a) *Msss* isomer; b) transition state of the M_1 isomerization from *Msss* to *Pssa*; c, d) transition state of the M_0 isomerization from *Msss* to *Psss*: c) view from above the oxygen atom, d) view from below the phosphorus atom with arrows representing the eigenvector related to the stereomerization mode.

can be observable by chromatographic methods at this temperature. Moreover, these results suggest that isolation of configurationally stable residual enantiomers could be feasible. It is also worth noting that **4a** and **4e** have similar M_0 barriers despite ethyl being significantly bigger than methyl, whereas when R is *i*Pr the barrier is ≈4.5 kcal mol^{-1} larger. This can be explained by inspecting the molecular structural changes occurring upon reaching the transition state, as detailed below.

Some B3LYP/cc-pVDZ selected structures of **4f** are reported in Figure 1. The main structural features of the *sss* isomers of **4a**, **4e**, and **4f** do not significantly depend on the R substituent: the C–P bond length is 1.82 Å, the C-P-C angle is 108°, and the aromatic moieties make an angle of about 35° with the P=O bond. At the corresponding M_0 transition state, the angle between the aromatic moieties is evidently close to 0°, the C-P-C angle is 112°, and the C–P bond length is 1.86 Å. As before, these length and angles negligibly depend on the substituent R. Therefore, for systems differing by an *ortho* substituent only, such as **4a**, **4e**, and **4f**, the unequal heights of the activation barriers do not depend on the deformation about the central phosphorus atom. The nature and components of the eigenvector related to the reactive mode with negative curvature (Figure 1 d) indicate that the crucial region of the M_0 transition state is that below the P=O moiety in which the aromatic rings come to a close contact. Indeed, the hydrogen atoms in the 4-position of the indole moiety are as close as 1.79 Å in **4a** and **4e**, and 1.77 Å in **4f**, that is, less than twice the hydrogen van der Waals radius (1.0 ± 0.1 Å).[18] This causes a small deviation from planarity of the indole rings at the transition state of **4a** and **4e**, about 1° and 3° respectively, but is as large as 17° at the transition state of **4f**. Thus, the substituent-induced difference in the activation barriers can be traced back to a larger deviation from planarity of the aromatic moieties due to the increased size of the R substituent, which pushes the portions of the aromatic rings close to the phosphorus apart and forces the lower portions to come into contact. This can be illustrated by the variation of several geometric parameters in the M_0 transition state, for example, the angle P-C_3-C_{3a} is 134.2, 134.3, and 132.9° in **4a**, **4e**, and **4f**, respectively.

To investigate the possibility of resolving the residual racemates by chiral reverse-phase HPLC analysis, we also performed PCM calculations to estimate the solvent effect of an acetonitrile/water 1:3 mixture on the energetics of these phosphane oxides. The results of PCM-B3LYP calculations using averaged solvent parameters are marginally different from those obtained by averaging the results for pure acetonitrile and pure water.

Inclusion of the solvent effects due to the acetonitrile/water 1:3 mixture at the PCM-B3LYP/cc-pVDZ level reduces the differences between the minimum energy structures by 1–2 kcal mol^{-1}. Even if the energetic change is rather small in absolute, this change has a large effect on the stereoisomer population, because it is a significant fraction of the energy difference. As a consequence, the molar fraction of the *ssa* stereoisomers becomes significant (25-32 %), whereas the *saa* and *aaa* isomers are in the small percentage range. This behavior indicates that the isomer energy differences are based on electrostatic interactions in addition to steric repulsion interactions. Inclusion of the solvents effects leads to a decrease in the stereomerization activation barriers amounting to 0–1 kcal mol^{-1} for the M_0 processes and to 2–3 kcal mol^{-1} for the M_1 processes. The barrier height change due to solvent effects is again rather small,

but now also in a relative sense, especially for M_0 barriers (<5%). For M_0 stereomerizations, steric repulsion is the major contribution to the activation barrier, as discussed above.

Thus, the presence of the polar acetonitrile/water 1:3 mixture largely affects the isomer populations, makes the diastereomerization within the residual enantiomers sets faster, and leaves approximately unchanged the enantiomerization rate between residual enantiomers.

In conclusion, the picture arising from the computational results is that 1) *P*/*Msss* are by far the major isomers present, 2) M_1 diastereomerization within each residual enantiomer is fast at room temperature, and 3) residual enantiomers should undergo rather slow M_0 enantiomerization at room temperature.

Synthesis of phosphane oxides 4 and 5: Phosphorus oxybromide reacts with 1,2-disubstituted indoles in dry pyridine, directly affording tris(3-indolyl)phosphane oxides **4a** and **4c**–**4f**. By using 2-methylbenzimidazole as a substrate, **5** is obtained in good yields. In the synthesis of **4e**, we observed that significant amounts of the C_1-symmetric phosphane oxide **4h**, isolated by chromatography, were formed if the starting 2-ethyl-1-methylindole contained some 1-methylindole. Compound **4h** could be obtained in good yields by using a 2:1 mixture of 2-ethyl-1-methylindole and 1-methylindole.

The reaction of **4c** with boron tribromide in methylene dichloride afforded the tris[3-(2-bromomethyl-1-methyl)indolyl]phosphane oxide (**4g**), which was converted, in a crude state, into **4b** in quantitative yields by reaction with lithium aluminium tetradeuteride in THF.

Characterization of phosphane oxides 4 and 5: All of the tris(3-indolyl)phosphane oxides **4** and the benzimidazole derivative **5** were characterized on the basis of their analytical and spectral data, in particular ^{1}H NMR and MS spectra. A single enantiomeric couple (presumably *Psss*/*Msss*) was invariably detected by ^{1}H NMR spectroscopy down to −90 °C in all cases.

As for the single crystal XRD structures, the data are now available for all compounds, except for **4b**, the trisdeuterated form of **4a**, and **4g**, which was isolated only in a crude state as an intermediate for the synthesis of **4b**. The XRD structures of **4c**, **4h**, and **5** are shown in Figure 2; those of **4a**, **4e**, and **4f** were previously published.[12]

In all cases both enantiomeric forms are present in the crystalline structure (the crystal space groups contain an inversion centre). The *Mssa* and *Pssa* are the main conformers populating the crystalline form of **4c** and **4h**, while the *Psss*/*Msss* are the sole isomers present in the case of **5**, in analogy with the structures found for **4a**, **4e**, and **4f**.

The hub–aryl bond length and the aryl-hub-aryl angle, which are relevant structural parameters directly influencing the gearing level of the blades, are summarized in Table 2.

It is interesting to note that the C-P-C angle value in **4c** and **4h** falls in the range of the classical values found for conformationally free unconstrained tris(aryl)phosphane oxides,[19] while it is definitely narrower in the case of **5**. Furthermore, the P–N bond length in **5** (1.67 Å) is much shorter than in the indole-based phosphane oxides **4** (1.78 Å), even though it is longer than the C_{sp^3}–N bond in **2** (1.45 Å).

The combination of these parameters suggests that they should synergistically cooperate to raise the configurational stability of the residual enantiomers, which should increase along the sequence **4a** < **5** < **2**, as a consequence of the parallel increase of the inter-ring gearing.

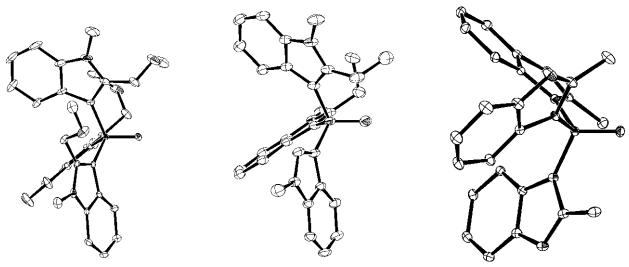

Figure 2. ORTEP presentations of a single enantiomer of: **4c** (left), **4h** (middle), and **5** (right).

Table 2. Structural parameters of three-bladed molecular propellers from XRD data.

Substrate	Hub–Aryl bond length [Å][a]	Aryl-Hub-Aryl angle [°][a]
4a	1.781	107.1
4c	1.795	106.8
4e	1.777	106.7
4f	1.779	106.9
4h	1.773	107.2
5	1.674	105.4
2	1.448	111.9
3	1.441	117.3

[a] Mean value over the three blades

Resolution of the residual racemates of phosphane oxides 4, 5, and of tris[1-(2-methyl)benzimidazolyl]methane (2): Preliminary experimental evidence for the existence of tris[3-(1,2-dimethyl)indolyl]phosphane oxide **4a** as a couple of residual enantiomers was given by ^{1}H NMR analysis. Progressive addition of europium tris[3-(eptafluoropropyl-hydroxymethylene)-(+)-camphorate] to a solution of **4a** in $CDCl_3$ produced clear splitting of the sharp signal attributable to the methyl group in the 1-position of the indole rings. The same effect was observed by treating the solution of **4a** in $CDCl_3$ with an equimolar amount of (+)-Naproxen. Surprisingly, in both cases, the *N*-Me singlet was the only signal to undergo splitting under the effect of these chiral additives. The experimental proof for the existence of **4a** as a couple of residual enantiomers was achieved by CD and UV-detected chiral stationary phase (CSP) HPLC (ChromTech, Chiral AGP 100×4.0 mm, 5 μm; eluant: acetonitrile/K_2HPO_4 buffer (pH 4.5, 1 mg mL^{-1}) 3:1). A plateau interconnecting the peaks in the UV-detected chromatogram at room temperature suggested that the enantiomerization process is

active at this temperature, even though at a quite slow rate.[12]

A very similar behavior was shown by the tris[3-(2-methoxymethyl-1-methyl)indolyl]phosphane oxide (**4c**). A plateau between the peaks of the enantiomers was clearly visible in the chromatogram at room temperature, indicating that slow interconversion of the antipodes was occurring during elution (see below).

CSP HPLC experiments performed on **4e** demonstrated that complete analytical resolution was achieved In this case, the difference in the retention times of the residual antipodes was about four minutes (Figure 3a, black curve).

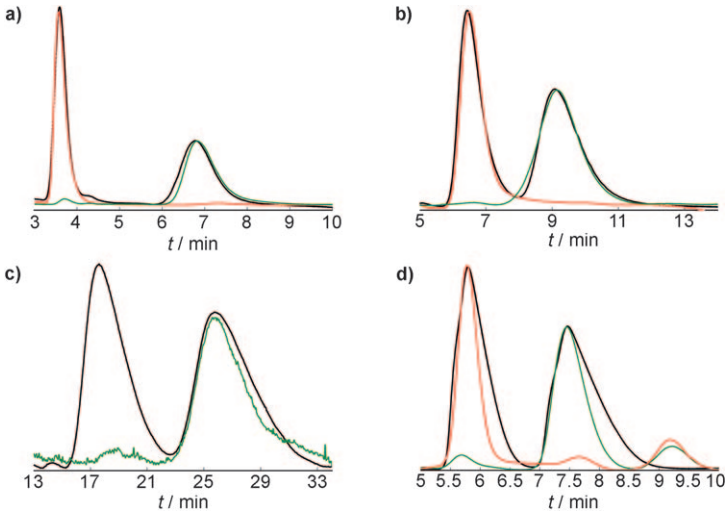

Figure 3. CSP HPLC chromatograms and enantiomeric purity control of the residual enantiomers obtained from semipreparative HPLC resolution on chiral stationary phase: black line: residual racemate, red line: first eluted residual enantiomer; green line: second eluted residual enantiomer. a) **4e**, b) **4f**, c) **5**, d) **2**. An achiral impurity, formed during the chromatographic resolution process together with 2-methylbenzimidazole, is visible at about 9 min. elution time.

The resolution process was scaled to semipreparative level and solutions of nearly enantiopure residual enantiomers in the eluant were isolated. The first eluted dextrorotatory enantiomer was obtained with an enantiomeric ratio (e.r.) larger than 97.5:2.5 (Figure 3a, red curve), while the more retained levorotatory isomer displayed an e.r. of about 95.0:5.0 (Figure 3a, green curve).

The removal of one of the three *ortho* ethyl groups from **4e** produced the total loss of configurational stability at room temperature. Attempts to resolve **4h** into antipodes by CSP HPLC, under the experimental conditions which so efficiently resolved all the indole-based phosphane oxides investigated in this paper, were unsuccessful.

This result emphasizes the importance of the bulkiness of the *ortho* substituents in developing an efficient correlated rotation of the rings. As expected, an increase in the size of the *ortho* alkyl group from ethyl to isopropyl favourably affected the configurational stability of the residual enantiomers.

We were able to analytically resolve the residual racemate of phosphane oxide **4f**, even though the difference in the retention times of the antipodes was not as high as in the case of **4e** (Figure 3b, black curve). Also in this case, we obtained some milligrams of almost enantiopure residual antipodes of **4f** by semipreparative CSP HPLC: the first eluted enantiomer was found to be dextrorotatory (589 nm, CH_2Cl_2) and was isolated in a 99.9:0.1 e.r. (Figure 3b, red curve), while the e.r. of the second eluted levorotatory enantiomer was 98.5:1.5 (Figure 3b, green curve).

The CSP HPLC resolution of the residual racemate of **5** was found more difficult than those previously performed in the case of the indole-based phosphane oxides, due to the small difference in the retention times of the antipodes (Figure 3c, black curve). Only the more retained levorotatory antipode could be isolated in a good enantiomeric purity level (e.r $\approx$98.7%, Figure 3c, green curve).

As anticipated, we also tried to resolve the already known tris[1-(2-methyl)benzimidazolyl]methane (**2**), since we considered essential that the experimental conditions employed for evaluating the configurational stability would be as similar as possible for all the substrates. The CSP HPLC resolution of racemic **2**, prepared according to the procedure described in the literature,[11] was rather troublesome, due again to the small difference in the retention times of the antipodes. Attempts to reproduce the chromatographic methodology described in literature (repeated medium-pressure chromatographic processes on microcrystalline cellulose triacetate with 95% ethanol as eluant) failed, since the eluted products showed an unsatisfactory enantiomeric purity. In addition, some degradation of the starting material was observed. A nearly enantiopure sample of both enantiomers was obtained by employing a mixture of MeCN and sodium acetate buffer (pH 4.5) in a 15:85 ratio. A more retained achiral impurity, probably resulting from the loss of one benzimidazole unit, was present in the resolved enantiomers. The first eluted dextrorotatory enantiomer was obtained with an e.r of 94.5:5.5 (Figure 3d, red curve), while an e.r. of 93.5:6.5 was found for the second eluted antipode (Figure 3d, green curve).

Evaluation of the enantiomerization barriers of residual enantiomers: For the quantitative evaluation of the thermodynamic parameters involved in the enantiomerization process of the residual enantiomers, three techniques were considered: CD decay kinetics, dynamic CSP HPLC, and dynamic ^{1}H NMR spectroscopy.

For all techniques, the measurement at a single temperature provides one rate constant (we assume that enantiomerization is a first-order process). By measuring the temperature dependence of the rate constant, the activation enthalpy and entropy for the enantiomerization process are obtained. To improve the statistical reliability, this conventional two-step procedure has been substituted by a one-step procedure featuring the simultaneous fitting of all variable-temperature data to an appropriate model and resulting in the desired thermodynamic parameters. It should be noted

that the CD signal is proportional to the enantiomeric purity, so its exponential decay directly provides the desired rate constant. Conversely, to extract the rate constant from the CSP HPLC or NMR profiles one needs to formulate a model and to fit the latter to the experimental data. This indirect method may affect the accuracy of the thermodynamic parameters so obtained.

The most appropriate technique was selected on the basis of the configurational stability of the compound to be studied. When the residual enantiomers were stable enough at room temperature to be obtained in an acceptable purity level by semipreparative CSP HPLC, the measurement of CD decay kinetics at different temperatures was chosen as the most direct and reliable method. The CD measurements were carried out for **2**, **4e**, **4f**, and **5** in MeCN/water mixtures similar to those used as eluant for the semipreparative resolution process and for the CSP DHPLC experiments (see Experimental Section). The experimental and best-fit CD decays of **2** and **4e** are shown in Figure 4.

When the residual enantiomers were found too labile to survive at room temperature for at least for a week, the CSP DHPLC method was considered as the second choice system for acceding to reliable barrier values. This technique has been applied to **4a**[12] and **4c** (Figure 5); it was also applied to **4e** for the sake of comparison, even though complete coalescence could not be attained. The most strict limitation of this technique is the rather narrow temperature range sustainable by the chiral stationary phase, which undergoes degradation at about 65 °C. Another point which deserves consideration, differentiating this technique from CD and NMR based methods, is the presence of a chiral enantiopure species, the stationary phase, which could, in principle, influence the path of the enantiomerization process.

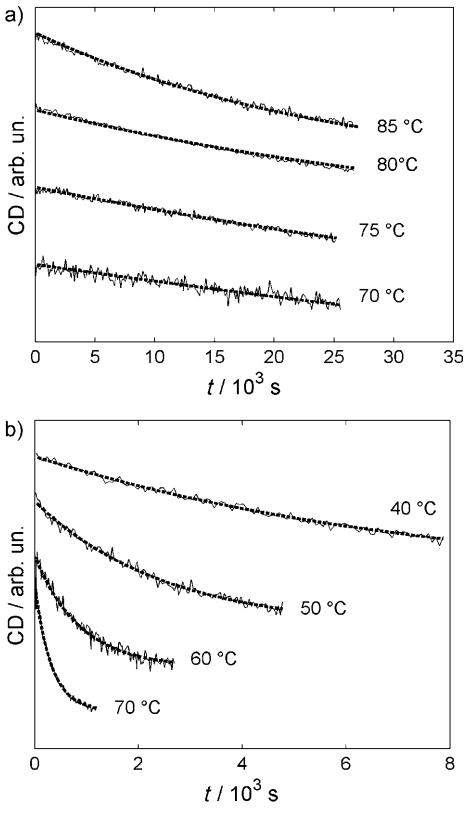

Figure 4. Variable-temperature CD decays; thin solid line: experimental; thick dashed line: best-fit. Top: **2** (solvent MeCN:water/15:85). Bottom: **4e** (solvent MeCN:water/28:72). The CD curves have been vertically shifted for the sake of clarity. Note the different timescale in the two panels.

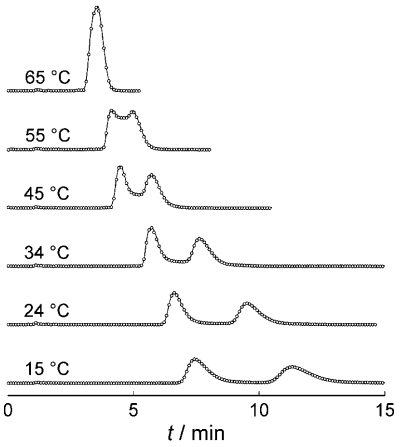

Figure 5. Variable-temperature dynamic CSP HPLC of **4c** (eluant MeCN/water 2:8, flow 0.7 cc min^{-1}); open circles: experimental; solid line: best-fit.

The DNMR technique was applied in the case of substrates displaying methylenic hydrogen atoms, like **4b**, **4c**, and **4d**, or methyl groups, like **4f**, which are diastereotopic and magnetically non-equivalent in the minimum energy states and in the TSs associated with the M_1 mechanism, whereas they are enantiotopic, that is, isochronous, in the C_{3v}- or C_s-symmetric TSs associated with the M_0 process.

Variable-temperature experiments could supply indications on the enantiomerization energetics. However, the solvent (generally [D$_6$]DMSO) and the concentration employed in ^{1}H NMR experiments are different from those used in CSP DHPLC and CD based kinetic work for solubility reasons. This constraint makes questionable the comparison of the data supplied by the DNMR spectroscopy with those obtained from the two other techniques. Furthermore, in some cases the signal pattern and its variations with temperature were not interpretable in full detail.

The thermodynamic parameters derived from the analysis of the CD decay and from fitting the CSP HPLC profiles are reported in Table 3.

In a single case, namely **4e**, it was possible to apply all of the three techniques, thus allowing us to assess their reliability and consistency. The activation enthalpy $\Delta H^{\neq}$ value is the same for both techniques within the estimated error, whereas the activation entropy $\Delta S^{\neq}$ is largely different notwithstanding solvent mixture and temperature range were very similar.

This discrepancy can be better understood by enlarging the view to all of the results reported in Table 3. It can be

Table 3. Experimental activation parameters for M_0 enantiomerization of C_3-symmetric tris(aryl)phosphane oxides **4a**, **4c**, **4e**, **4f**, **5**, and **2** obtained by CD and CSP DHPLC techniques.

System	Method	T [°C]	$\Delta H^{\neq}$ [kcal mol^{-1}]	$\Delta S^{\neq}$ [cal K^{-1} mol^{-1}]	$\Delta G^{\neq}$ (25 °C) [kcal mol^{-1}]
2	CD	70–85	27 ± 4	−4 ± 3	28 ± 1
4a[a]	CSP DHPLC	23–70	18 ± 1	−20 ± 4	25 ± 2
4c	CSP DHPLC	15-65	19.4 ± 0.4	−21.6 ± 0.3	26.0 ± 0.4
4e	CSP DHPLC	25–59	22.2 ± 0.1	−23.2 ± 0.1	29.1 ± 0.1
4e	CD	40–70	22.0 ± 0.5	−6 ± 2	23.8 ± 0.5
4f	CD	50–82	23 ± 2	−6 ± 5	25 ± 2
5	CD	50–80	14 ± 1	−38 ± 3	25 ± 1

[a] From reference [12].

seen that all $\Delta S^{\neq}$ values are negative, but the values from CSP DHPLC experiments are about −20 cal K^{-1} mol^{-1}, whereas those from CD decay experiments are only about −5 cal K^{-1} mol^{-1}, except for **5**. It is then reasonable to deduce that the activation entropy $\Delta S^{\neq}$ contains a sort of technique-related systematic error. Hence, the activation enthalpy $\Delta H^{\neq}$ values from CD decay and CSP HPLC experiments are consistent with each other, whereas the activation entropy $\Delta S^{\neq}$ (and then the activation free energy $\Delta G^{\neq}$) values are consistent only within a single technique.

As for dynamic NMR spectra, extensive fitting rounds of the NMR lineshapes showed that, owing to the limited affordable temperature range and the presence of temperature-dependent fitting parameters (chemical shifts), the fitted activation parameters are not accurate and statically reliable enough for the quantitative determination of the activation barriers. In the present case, dynamic NMR spectroscpopy can provide qualitative information on the configurational stability and an auxiliary consistency check of the activation barrier values obtained by CD decay or CSP HPLC. If the temperature-dependent NMR lineshapes can be satisfactorily fitted by fixing the activation parameters to those from CD decay or CSP HPLC and leaving the chemical shifts and J couplings only as free parameters, then the NMR data are consistent with the previously obtained activation parameters.

The activation enthalpy $\Delta H^{\neq}$, in the case of the indolyl phosphane oxides, grows in the sequence **4a** < **4c** < **4e** < **4f**, showing that the activation barrier in a series of homologue compounds in which the *ortho* substituent is an alkyl group is mainly affected by the steric hindrance. It is worth noting that the CH_2OMe substituent is effectively less hindering than ethyl (Table 3). The largest $\Delta H^{\neq}$ is shown by **2** despite the *ortho* substituent being methyl, probably because the aryl–hub distance is the shortest of the set (C–N bond). Compound **5**, which is similar, has the smallest $\Delta H^{\neq}$ and we will comment later about this somehow puzzling result.

On discussing the activation free energy $\Delta G^{\neq}$ at 25 °C (Table 3), it is worth recalling that differences in $\Delta G^{\neq}$ are only meaningful within a single experimental technique. As before, the $\Delta G^{\neq}$ increases as the *ortho* substituent becomes more hindering (**4a** < **4c** < **4e** by CSP HPLC; **4e** < **4f** by CD decay). Considering the CD results only, the activation barrier increases in the order **4e** < **4f** ~ **5** < **2**, demonstrating the great influence exerted on configurational stability by the length of the bond connecting the hub to the blades: the shorter the bond the stronger the engagement and, by consequence, the higher the enantiomerization barrier. We also note that our results yield an activation free energy for **2** at 70 °C of 28 kcal mol^{-1}, in agreement with that reported in literature for the racemization process carried out in dimethoxyethane (28.4 kcal mol^{-1} at 70 °C).[11]

Finally, we admit that the activation parameters of **5** have a peculiar behavior that we are not able to explain. $\Delta H^{\neq}$ is lower than expected on the basis of the geometrical parameters, while $\Delta S^{\neq}$ is more negative than expected on the basis of the employed technique, and, conversely, $\Delta G^{\neq}$ at 298 K is just as expected on the basis of the relationship to the structurally related compound **2**.

We also carried out variable-temperature ^{1}H NMR experiments even though, as anticipated, these experiments can at most represent a consistency check of the enantiomerization barriers obtained from CD decay and CSP HPLC experiments. To investigate the enantiomerization dynamics of **4a** by ^{1}H NMR (or ^{2}H NMR) spectroscopy in addition to the CSP DHPLC technique, we prepared the tris[3-(2-monodeuteromethyl-1-methyl)indolyl]phosphane oxide (**4b**). We found, however, that the diastereotopic hydrogen atoms of the methylene groups of **4b** were magnetically isochronous in the ^{1}H NMR spectra recorded in different solvents even at very low temperatures.

The methylene protons of the methoxymethylene groups of **4c** gave rise to the AB system typical of two coupled diastereotopic protons at room temperature ([D$_6$]DMSO) (Figure 6). The activation parameters were fixed to the values from CSP HPLC, and ^{1}H NMR lineshapes were subjected to a constrained best-fit procedure. As shown in the right panel of Figure 6, the lineshape can be accurately fitted to the model and the best-fit spin parameters (ω_A = 4.64–4.67 δ, ω_B = 4.66–4.68 δ, J_{AB} = 12.1 Hz) are compatible with indolic methoxymethylene protons.

The decoupled signal of the methylene protons in the ^{1}H NMR spectra of **4e** ([D$_6$]DMSO) recorded at different temperatures (from 25 to 150 °C) does not undergo complete coalescence to a singlet even at high temperature.[12] Again, we fixed the activation parameters to those obtained by CSP HPLC or by CD decay and subjected the ^{1}H NMR lineshapes to a constrained best-fit procedure. The ^{1}H NMR spectra of **4e** prove to be consistent with the activation parameters derived from both CD decay and CSP HPLC and the goodness-of-fit measure and the best-fit spin parameters (ω_A = 2.98–3.02 δ, ω_B = 2.90–2.97 δ, J_{AB} = 14.0 Hz, J_{AX} = 7.4 Hz) are only marginally different.

Reduction of phosphane oxide 4e to tris[3-(2-ethyl-1-methyl)indolyl]phosphane (6): Since the chromatographic separa-

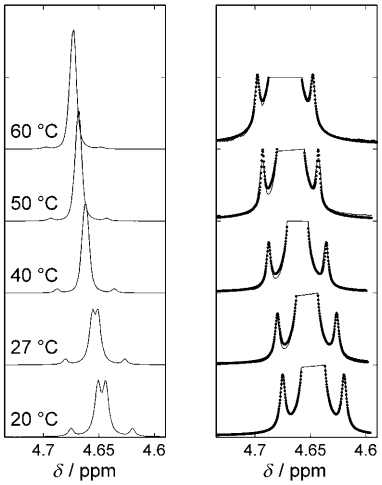

Figure 6. ^{1}H-DNMR experiments on **4c** ([D$_6$]DMSO). Left panel: experimental spectra of the methylene protons of the methoxymethylene groups. Right panel: enlarged view of the external minor peaks; line: experimental spectra, dots: constrained best-fit spectra.

tion of residual enantiomeric phosphanes is a problem that is still waiting for a satisfactory solution, a point deserving investigation was the reductive conversion of the most stable phosphane oxides, for example, **4e** and **4f**, into phosphanes and the evaluation of their configurational stability in comparison to the parent compounds.

The reduction of phosphane oxide **4e** to tris[3-(2-ethyl-1-methyl)indolyl]phosphane (**6**) was performed with an excess of trichlorosilane and triethylamine (TEA) in toluene under an argon atmosphere, according to a known procedure.[20] Lithium aluminum hydride, even if activated with trimethylsilyl chloride, showed a much lower reducing activity than trichlorosilane. Phosphane **6** was obtained in 40% isolated yield and was characterized on the basis of MS and NMR spectral data. It was found to be an extremely oxidizable compound and was easily converted into phosphane oxide **4e** by brief exposure to air even in the solid state.

The lowest reaction temperature necessary to observe an acceptable reaction rate for the reduction was found to be about 80°C, which was too high to reduce the enantiopure oxide to the enantiopure phospane without contemporary racemization. As anticipated, phosphane oxide **4e** was found to be configurationally quite stable at 25°C, while helix inversion was rather fast at 70°C. Thus, the reduction of an enantiopure sample of **4e** at 70°C unavoidably afforded racemic phosphane **6**.

We found phosphane oxide **4f** unreactive in the presence of lithium aluminum hydride and trichlorosilane, even when heated to reflux in mesitylene. The reason for this reactivity drop was attributed to the high hindrance exerted by the three isopropyl groups surrounding the central phosphorus atom.

Configurational stability of tris[3-(2-ethyl-1-methyl)indolyl] phosphane (6): The configurational stability of phosphane **6** was qualitatively assessed by ^{1}H NMR dynamic spectroscopy, the sole technique applicable on a racemate. The signals of the methylene protons appear as a sharp quartet, which is progressively converted into a complex broad multiplet by lowering the temperature. These observations indicate that, in the case of phosphane **6**, the enantiomerization process is fast even at room temperature.

There are at least two processes that can be envisaged as being responsible for the enantiomerization of the residual antipodes of phosphanes: helix reversal, produced by the M_0 mechanism or pyramidal inversion at the phosphorus centre. The latter mechanism causes enantiomerization, because it converts, for example, the *Msss* isomer into the *Maaa* isomer, which is one of the stereoisomers constituting the residual antipode.

This hypothesis looks credible on the basis of the consideration that dramatic changes in geometry on passing from phosphane oxides to phosphanes are not expected and, by consequence, also the level of ring engagement and the configurational stability should not be much different in phosphane and phosphane oxide. The extensive theoretical and experimental work reported in literature on the inversion barrier of trivalent phosphorus derivatives[21] suggests, however, that energies much higher than 20 kcal mol^{-1} are involved in the inversion processes of phosphanes, even though no specific data is available for tris(aryl)phosphanes.

To have a reliable indication on the more favorable enantiomerization path we resorted to a supplementary computational investigation of phosphane **6**. We computed the activation barriers for the two processes at the DFT-B3LYP/cc-pVDZ level, as performed for the corresponding phosphane oxide **4e**. The barrier for the inversion from *Msss* to *Maaa* was calculated to be 25.1 kcal mol^{-1} and that for the M_0 isomerization from *Msss* to *Psss* (and vice versa) amounted to 11.7 kcal mol^{-1}. The computational data thus suggest that the M_0 process is much faster than inversion and that the enantiomerization of **6** occurs through the M_0 mechanism, just as in the indolic phosphane oxides **4**. The calculations also indicate that the mechanical inter-ring gearing at the transition state is strongly diminished on passing from phosphane oxide **4e** to phosphane **6**. Indeed, the aromatic moieties of **6** can be considered planar, deviating by less than 0.5° from planarity, and the distance between the close-contact hydrogen atoms in the 4-position of the indole moieties is 1.90 Å in **6**, which is significantly longer than the 1.79 Å in **4e**. It seems that these differences are due to the presence of the oxygen atom in **4e** that pushes the portions of the aromatic rings close to the phosphorus apart, thus causing the nonplanar deformation of the aromatic rings.

Conclusions

This work reports some results that serve as a guide for designing configurationally stable C_3-symmetric propeller-shaped residual enantiomers. Several members of a series of molecular propellers with a non-invertible atom as the hub have been obtained as configurationally stable residual anti-

podes and their enantiomerization energy barriers have been evaluated by different techniques.

Even though a reliable comparison of the barriers was found possible only if the technique employed for their assessment is the same, the results of the research clearly demonstrate that three structural parameters are, in the main, responsible for the efficacy of the correlated rotation of the blades and consequently for the configurational stability of the residual antipodes: 1) the size of the substituents located in the *ortho* position on the aromatic rings, 2) the length of the bond connecting the central group, that is, the propeller hub, and the aromatic rings, and 3) the aryl-hub-aryl angle describing the pyramidality of the propeller.

The importance of the bulkiness of the *ortho* substituent is demonstrated by the experimental racemization energy barriers $\Delta G^{\neq}$ at 25 °C, which, according to the CSP HPLC experiments, progressively increase along the sequence **4a** (R = Me, $\Delta G^{\neq} = 25$ kcal mol^{-1}), **4c** (R = CH_2OMe, $\Delta G^{\neq} = 26$ kcal mol^{-1}), and **4e** (R = Et, $\Delta G^{\neq} = 29$ kcal mol^{-1}). The series is extendable to **4f** (R = *i*Pr) if the CD decay data of **4e** ($\Delta G^{\neq} = 23.8$ kcal mol^{-1}) and **4f** ($\Delta G^{\neq} = 25$ kcal mol^{-1}) are compared (Table 3). The resolution of the residual racemates into antipodes could be achieved at an analytical level in the case of **4a** and **4c**, which are configurationally labile at room temperature, and on a semipreparative scale in the case of **4e** and **4f**.

The relevance of the length of the bond connecting the central group and the aromatic rings is demonstrated by comparing the configurational stability of substrates exhibiting closely similar geometry of the blades, bearing identical *ortho* substituents (Me groups), but differing in this parameter. In the series of **2** (C_{sp^3}–N_{sp^2} bond length = 1.45 Å), **5** (P–C_{sp^2} bond length = 1.67 Å) and **4a** (P–C_{sp_2} bond length = 1.78 Å), configurational stability dramatically decreases from **2** ($\Delta G^{\neq} = 28$ kcal mol^{-1}, CD decay) to **5** ($\Delta G^{\neq} = 25$ kcal mol^{-1}, CD decay), which is stable at 25 °C, to **4a**, which undergoes fast racemization at room temperature.

More complex is the quantitative evaluation of the effects of the aryl-hub-aryl angle. Even though not fully comparable, since obtained on structurally different substrates and under different experimental conditions, the dramatically different stereomerization barriers for **3** (117.3°, $\Delta G^{\neq} = 17.7$ kcal mol^{-1} at −21 °C, determined by ^{1}H NMR experiments)[8] and **4a–4f** (about 106–107°, $\Delta G^{\neq} = 20$–30 kcal mol^{-1} at 25 °C) demonstrate that this parameter strongly influences the correlated rotation of the rings.

The nature of the atom constituting the propeller hub probably exerts the most important effect on the stability of residual enantiomeric propellers, since it controls all the three parameters discussed above.

An unexpected difficulty in designing stable residual enantiomeric phosphanes, similarly to amines, was found to be related to the lack of an apical group on the central atom above the reference plane. Such an apical group seems to play a very important role on the M_0 mechanism barrier; phosphorus pyramidal inversion seems a less probable racemization path.

A new steric and electronic design of the blades is required to accede to C_3-symmetric stable tris(aryl)phosphanes that can be used as mediators in catalysis: 1) the phosphorus center should not be overcrowded by too bulky *ortho* substituents, which would preclude complexation with a metal; and 2) the influence of the electronic availability at the phosphorus atom on configurational stability must be investigated and electronically tailored blades made available.

Experimental Section

Organic synthesis: $[\alpha]_D$ were recorded with a Jasco P-1030 polarimeter. CD spectra and dichroism decay experiments were recorded with a Jasco P-810 spectropolarimeter provided with a temperature-controlled probe Peltier Jasco PFD 425S. CSP HPLC analyses and semipreparative separations were performed on a Waters 600E instrument equipped with a UV detector Waters 486 and recorded at 220 nm. Analytical column: CromTech CHIRAL-AGP column (100 × 4.0 mm, 5 μm); loop: 20 μL; substrate concentration: 1 mg mL^{-1}; Semipreparative column: CromTech CHIRAL-AGP column (150 × 10.0 mm, 5 μm); loop: 500 μL. NMR spectra were recorded on Bruker AV 400 and Bruker AC 300 spectrometers. Mass spectra were recorded on Bruker Daltonics high resolution FT-ICR (Fourier Transform Ion Ciclotron Resonance) model APEXTM II (4.7 Tesla Magnex cryomagnet supplied with ESI source) and Thermofiningan LCQ Advance (APCI). Purification by column chromatography was performed by using Merck silica gel 60 (230–400 mesh for flash-chromatography and 70–230 mesh for gravimetric chromatography). 1,2-Dimethylindole and 1-ethyl-2-methylindole were bought from Sigma Aldrich and were used as received. 1-Methyl-2-methoxymethylindole was synthesized by alkylation of the 2-hydroxy-1-methylindole, prepared in turn by reaction of the lithium derivative of 1-methylindole with formaldehyde as described below.

2-Hydroxymethyl-1-methylindole: A 1.6 M solution of *n*BuLi in hexane (32 mL, 50 mmol) was added to a solution of *N*-methylindole (5.0 g, 38 mmol) in THF (40 mL) and the reaction mixture was heated to reflux for 3 h under a nitrogen atmosphere. After cooling to 0 °C, gaseous formaldehyde, produced by pyrolysis of paraformaldehyde (5.0 g), was bubbled through the reaction mixture, which was then stirred at room temperature for 1 h. The solvent was evaporated under reduced pressure, then CH_2Cl_2 (20 mL) and water (20 mL) were added. The organic phase was separated and dried over Na_2SO_4. The solvent was evaporated to dryness to give a residue that was purified by crystallization from diisopropyl ether (4.9 g, 80 %). ^{1}H NMR (300 MHz, $CDCl_3$): $\delta = 7.60$ (d, ^3J(H,H) = 8 Hz, 1H), 7.35 (d, ^3J(H,H) = 8 Hz, 1H), 7.26 (m, 1H), 7.13 (m, 1H), 6.48 (s, 1H), 4.83 (s, 2H), 3.83 ppm (s, 3H).

1-Methyl-2-methoxymethylindole: 2-Hydroxymethyl-1-methylindole (2.7 g, 17 mmol) was added to a 60 % suspension of NaH (0.9 g, 38 mmol) in MeCN (50 mL). After stirring for 1 h at 50 °C, CH_3I (1.6 mL, 26 mmol) was added and the reaction mixture heated at 30 °C for 2 h. A second portion of CH_3I (1.6 mL, 26 mmol) was added and the reaction mixture stirred for 12 h. The solvent was evaporated to dryness and the residue was subjected to column chromatography (silica gel, CH_2Cl_2) to give 1-methyl-2-methoxymethylindole (1.14 g, 39 %). M.p. 65 °C; ^{1}H NMR (400 MHz, $CDCl_3$): $\delta = 7.60$ (dt, ^3J(H,H) = 8.0 Hz, ^4J(H,H) = 0.85 Hz, 1H), 7.33 (dd, ^3J(H,H) = 8.0 Hz, ^4J(H,H) = 0.85 Hz, 1H), 7.23 (m, 1H), 7.10 (m, 1H), 6.49 (s, 1H), 4.62 (s, 1H), 3.78 (s, 1H), 3.35 ppm (s, 1H).

Tris[3-(2-methoxymethyl-1-methyl)indolyl]phosphane oxide (4c): A solution of 2-methoxymethyl-1-methylindole (1.1 g, 6.3 mmol) in pyridine (2 mL) was added to a mixture of $POBr_3$ (0.56 g, 2 mmol) and pyridine (2 mL) under a nitrogen atmosphere. After stirring overnight at 90 °C, CH_2Cl_2 was added and the organic layer was washed with a 1 N HCl solution, dried (Na_2SO_4), and concentrated under reduced pressure. Purification of the residue by chromatography (silica gel, CH_2Cl_2/MeOH 9.5:0.5)

yielded **4c** (0.65 g, 20%). M.p. 182°C; ^{1}H NMR (300 MHz, $CDCl_3$): δ = 7.34 (d, ^3J(H,H) = 8.46 Hz, 1H), 7.14 (t, ^3J(H,H) = 7.63 Hz, 1H), 6.87 (d, ^3J(H,H) = 8.09 Hz, 1H), 6.77 (t, ^3J(H,H) = 7.53 Hz, 1H), 4.88 (d, ^2J-(H,H) = 12.8 Hz, 1H), 4.81 (d, ^2J(H,H) = 12.8 Hz, 1H), 3.84 (s, 3H; N-CH_3), 3.02 ppm (s, 3H; -O-CH_3); ^{13}C NMR (300 MHz, $CDCl_3$): δ = 143.58 (d, ^2J(C,P) = 18.7 Hz), 138.22 (d, ^3J(C,P) = 11.7 Hz), 128.54 (d, ^2J(C,P) = 11.7 Hz), 122.87 (s), 121.87 (s), 121.31 (s), 109.77 (s), 108.62 (d, ^1J(C,P) = 130.6 Hz), 64.54 (s), 58.07 (s), 30.95 ppm (s); ^{31}P NMR (300 MHz, $CDCl_3$): δ = 6.32 ppm (s); MS (APCI): *m/z* calcd for $C_{33}H_{36}N_3OP$: 569.6; found: 570.0 $[M+1]^+$; analytical HPLC retention times: 6.6 and 9.5 min; eluant MeCN/H_2O 20:80, flow rate 0.7 mL min^{-1}.

Tris[3-(1-ethyl-2-methyl)indolyl]phosphane oxide (4d): A mixture of $POBr_3$ (1.6 g, 5.5 mmol) and pyridine (2 mL) was added to a solution of 1-ethyl-2-methylindole (3.7 g, 23 mmol) in pyridine (2 mL) under nitrogen. The reaction mixture was heated at 60°C under stirring for 5 h, then diluted with dichloromethane and the resulting solution exhaustively extracted with a solution of 1N HCl. The organic layer was dried over Na_2SO_4 and evaporated to dryness to give a residue, which was subjected to chromatography (silica gel, CH_2Cl_2/MeOH 9.5:0.5). The first product eluted was some unreacted 1-ethyl-2-methylindole; the second product eluted was the tris[3-(1-ethyl-2-methyl)indolyl]phosphane oxide (**4d**) (2.6 g, 30%). M.p. 222°C; ^{1}H NMR (300 MHz, $CDCl_3$): δ = 7.31 (d, ^3J-(H,H) = 8.09 Hz, 1H), 7.06 (td, ^3J(H,H) = 7.53 Hz, ^4J(H,H) = 1.1 Hz, 1H), 6.70 (td, ^3J(H,H) = 7.53 Hz, ^4J(H,H) = 1.1 Hz, 1H), 6.54 (d, ^3J(H,H) = 8.09 Hz, 1H), 4.19 (q, ^3J(H,H) = 7.17 Hz, 2H), 2.57 (d, ^4J(H,P) = 1.1 Hz, 3H), 1.37 ppm (t, ^3J(H,H) = 7.17 Hz, 3H); ^{13}C NMR (300 MHz, $CDCl_3$): δ = 145.17 (d, ^2J(C,P) = 18.2 Hz), 136.55 (d, ^3J(C,P) = 11.4 Hz), 129.32 (d, ^2J(C,P) = 12.1 Hz), 121.31 (s), 120.79 (s), 120.60 (s), 109.32 (s), 105.73 (d, ^1J(C,P) = 132.8 Hz), 38.21 (s), 15.46 (s), 12.47 ppm (s); ^{31}P NMR(300 MHz, $CDCl_3$): δ = 7.98 ppm (s); MS (APCI): *m/z* calcd for $C_{33}H_{36}N_3OP$: 521; found: 522.2 $[M+1]^+$.

Bis[3-(1-methyl-2-ethyl)indolyl]-[3-(1-methyl)indolyl]phosphane oxide (4h): A solution of 2-ethyl-1-methylindole (8.8 g, 56 mmol) and 1-methylindole (2.9 g, 22 mmol) in pyridine (6 mL) was added to a mixture of $POBr_3$ (6.0 g, 21 mmol) and pyridine (6 mL) under a nitrogen atmosphere. After stirring 12 h at 90°C, CH_2Cl_2 was added and the organic layer was washed with a solution of 1N HCl, dried (Na_2SO_4), and concentrated under reduced pressure. The residue was purified by column chromatography (silica gel, CH_2Cl_2/MeOH 9.5:0.5). The first fraction eluted gave some unreacted 2-ethyl-1-methylindole (5.71 g, 35.9 mmol). The second fraction yielded the tris[3-(1-methyl-2-ethyl)indolyl]phosphane oxide (**4e**) (0.60 g, 1.15 mmol). The last fraction eluted gave the bis[3-(2-ethyl-1-methyl)indolyl]-[3-(1-methyl)indolyl]phosphane oxide (**4h**) (1.40 g, 2.83 mmol). M.p. 171°C ;^{1}H NMR (300 MHz, $CDCl_3$): δ = 7.81 (d, ^3J(H,H) = 7.97 Hz, 1H), 7.28 (m, 4H), 7.07 (m, 4H), 6.89 (d, ^3J-(H,H) = 7.92 Hz, 2H), 6.78 (t, ^3J(H,H) = 7.51 Hz, 2H), 3.72 (s, 9H), 3.29 (sextet, ^3J(H,H) = 7.34 Hz, ^2J(H,H) = 15.87 Hz, 2H), 3.13 (sextet, ^3J-(H,H) = 7.34 Hz, ^2J(H,H) = 15.87 Hz, 2H), 1.07 ppm (t, ^3J(H,H) = 7.44 Hz, 6H); ^{13}C NMR (300 MHz, $CDCl_3$): δ = 150.46 (d, ^2J(C,P) = 18.82 Hz), 138.05 (d, ^2J(C,P) = 10.17 Hz), 137.32 (d, ^3J(C,P) = 11.19 Hz), 135.32 (d, ^2J(C,P) = 21.37 Hz), 129.58 (d, ^2J(C,P) = 9.66 Hz), 128.66 (d, ^2J-(C,P) = 12.21 Hz), 122.40 (s), 122.33 (s), 120.99 (s), 120.74 (s), 120.63 (s), 120.28 (s), 110.32 (d, ^1J(C,P) = 128.69 Hz), 109.34 (s), 108.84 (s), 104.23 (d, ^1J(C,P) = 132.75 Hz), 33.03 (s), 29.43 (s), 19.11 (s), 13.77 ppm (s); ^{31}P NMR(300 MHz, $CDCl_3$): δ = 7.24 ppm (s); MS (APCI): *m/z* calcd for $C_{31}H_{32}N_3PO$: 494; found: 495.2 $[M+1]^+$.

Tris[3-(2-bromomethyl-1-methyl)indolyl]phosphane oxide (4g): A solution of BBr_3 (1M, 0.53 mmol) in CH_2Cl_2 (0.5 mL) was added to a solution of **4c** (0.10 g, 0.18 mmol) in CH_2Cl_2. The reaction mixture was stirred for 3 h and then diluted with water. The organic layer was separated, dried (Na_2SO_4), and concentrated under reduced pressure to give **4g**, which, due to its instability, was employed in a crude state without further purification (0.12 g; 95%); ^{1}H NMR (200 MHz, $CDCl_3$): δ = 7.36 (d, ^3J(H,H) = 8.33 Hz, 1H), 7.20 (t, ^3J(H,H) = 7.6 Hz, 1H), 6.97 (d, ^3J(H,H) = 7.9 Hz, 1H), 6.82 (t, ^3J(H,H) = 7.6 Hz, 1H), 4.97 (s, 2H), 3.84 ppm (s, 3H); ^{13}C NMR (300 MHz, $CDCl_3$): δ = 142.09 (d, ^2J(C,P) = 18.7 Hz), 138.47 (d, ^3J(C,P) = 11.7 Hz), 128.36 (d, ^2J(C,P) = 11.7 Hz), 123.77 (s), 122.06 (s), 121.90 (s), 110.05 (s), 107.13 (d, ^1J(C,P) = 131.5 Hz), 30.45 (s), 23.14 ppm (s); ^{31}P NMR(300 MHz, $CDCl_3$): δ = 5.76 ppm (s); MS (APCI): *m/z* calcd for $C_{30}H_{27}Br_3N_3OP$: 716; found: 717.8 $[M+1]^+$.

Tris[3-(2-deuteromethyl-1-methyl)indolyl]phosphane oxide (4b): A solution of **4g** (0.10 g, 0.14 mmol) in THF (10 mL) was added to a suspension of $LiAlD_4$ (0.010 g) in THF (1 mL), and the reaction mixture stirred for 30 min at 25°C. A 32% NaOH solution (0.1 mL) was added and the inorganic salts were removed by filtration. The filtrate was concentrated under reduced pressure and the residue was purified by chromatography (silica gel, CH_2Cl_2/MeOH 9.5:0.5) to yield **4b** (quantitative yield); ^{1}H NMR($CDCl_3$, 300 MHz): δ = 7.29 (d, ^3J(H,H) = 7.49 Hz, 1H), 7.08 (t, ^3J(H,H) = 7.49 Hz, 1H), 6.71 (t, ^3J(H,H) = 7.76 Hz, 1H), 6.65 (d, ^3J-(H,H) = 8.25 Hz, 1H), 3.71 (s, 3H), 2.55 ppm (br d, ^4J(H,P) = 1.56 Hz, 2H); ^{31}P NMR: δ = 8.34 ppm (s); MS (APCI): *m/z* calcd for $C_{30}H_{27}D_3N_3PO$: 482; found: 483.1 $[M+1]^+$.

Analytical HPLC resolution of tris[3-(2-ethyl-1-methyl)indolyl]phosphane oxide (4e): (+)-**4e**, 97.5:2.5 e.r, retention time 3.6 min; (−)-**4e**, 95:5 e.r., retention time 6.8 min; eluant MeCN/H_2O 30:70; flow rate 0.6 mL min^{-1}; semipreparative HPLC: (+)-**4e**, retention time 4.0 min; (−)-**4e**, retention time 6.8 min; eluant MeCN/H_2O 28:72; flow rate 4 mL min^{-1}.

Tris[1-(2-methyl)benzimidazolyl]phosphane oxide (5): A solution of $POBr_3$ (2.2 g, 7.6 mmol) in pyridine (15 mL) was rapidly added to a mixture of 2-methylbenzimidazole (3.1 g, 23.5 mmol) in pyridine (30 mL) under a nitrogen atmosphere. After 5 h stirring at 80°C, most of the solvent was removed under reduced pressure. $CHCl_3$ (25 mL) was added to the residue and the organic layer were washed with a 5% HCl solution, dried ($MgSO_4$), and concentrated under reduced pressure to yield pure **5** (2.0 g, 60%) as a white solid. M.p. 190–192°C; ^{1}H NMR (300 MHz): δ = 7.8 (d, ^3J(H,H) = 7.89 Hz, 1H), 7.32 (t, ^3J(H,H) = 7.87 Hz, 1H), 7.01 (t, ^3J-(H,H) = 8.37 Hz, 1H), 6.10 (d, ^3J(H,H) = 8.35 Hz, 1H), 2.54 ppm (s, 3H); ^{13}C NMR (400 MHz, $CDCl_3$): δ = 154.29 (s), 143.85 (s), 134.89 (s), 126.19 (s), 125.74 (s), 121.10 (s), 111.98 (s), 17.49 ppm (s); ^{31}P NMR(300 MHz, $CDCl_3$): δ = −15 ppm (s); MS (ESI): *m/z* calcd for $C_{24}H_{21}N_6PO$: 440; found: 441.16 $[M+H]^+$; analytical HPLC: (+)-**5** retention time 17.6 min; (−)-**5** retention time 25.8 min; eluant MeCN/H_2O 9:91; flow rate 0.8 mL min^{-1}; semipreparative HPLC: (+)-**5**, retention time 9.4 min; (−)-**5**, retention time 11.0 min; eluant MeCN/H_2O 15:85; flow rate 4 mL min^{-1}.

Tris[3-(2-ethyl-1-methyl)indolyl]phosphane (6): All the manipulations were performed under argon by using standard Schlenck techniques. $HSiCl_3$ (0.9 mL) was added to a solution of **6** (0.20 g, 0.38 mmol) and TEA (1.0 mL) in degassed toluene (5 mL) and the resulting suspension stirred at 80°C under argon for 5 h. A 10% NaOH solution (1 mL) was added at 0°C to the reaction mixture, and the organic layer was separated, dried, and concentrated under reduced pressure to give a residue, which was subjected to chromatography (silica gel, CH_2Cl_2/AcOEt 8:2). The first fraction eluted yielded **6** (0.080 g, 40%); ^{1}H NMR (300 MHz): δ = 7.23 (d, ^3J(H,H) = 8.2 Hz, 1H), 6.98 (m, 2H), 6.68 (m, 1H), 3.68 (s, 3H), 2.97 (q, ^3J(H,H) = 7.1 Hz, 2H), 0.96 ppm (t, ^3J(H,H) = 7.1 Hz, 3H); ^{13}C NMR (300 MHz, $CDCl_3$): δ = 147.04 (d, ^2J(C,P) = 37.06 Hz), 137.70 (s), 131.23 (s), 121.44 (s), 120.24 (s), 119.25 (s), 108.32 (s), 102.62 (s), 29.61 (s), 19.08 (d, ^3J(C,P) = 14.75 Hz), 13.78 ppm (s); ^{31}P NMR (300 MHz, $CDCl_3$): δ = −79.77 ppm (s); MS (EI): *m/z* calcd for $C_{33}H_{36}N_3P$: 505; found: 505 $[M]^+$.

Tris[1-(2-methyl)benzimidazolyl]methane (2):[11] Analytical CSP HPLC: (+)-**2**, 89% *ee*, retention time 5.8 min; (−)-**2**, 87% *ee*, retention time 7.5 min; eluant: MeCN/aqueous sodium acetate buffer 10 mM, pH 4.50–10/90; flow rate 0.8 mL min^{-1}; semipreparative CSP HPLC: (+)-**2**, retention time 7.2 min; (−)-**2**, retention time 8.8 min; eluant MeCN/aqueous sodium acetate buffer 15:85, 10 mM, pH 4.50; flow rate 4 mL min^{-1}. The pH of the solutions of the two residual enantiomers, collected in separated vials, were adjusted to neutrality with $NaHCO_3$, then $CHCl_3$ and NaCl were added and the organic layer separated, dried on Na_2SO_4 and the solvent removed under reduced pressure, giving yellowish residues of **2** (95% purity, HPLC).

Crystallographic data: CCDC-695918 (**4h**), 695919 (**4c**) and 695920 (**5**) contain the supplementary crystallographic data for this paper. These

data can be obtained free of charge from The Cambridge Crystallographic Data Centre via www.ccdc.cam.ac.uk/data_request/cif.

Acknowledgements

This work was supported by MIUR: FIRB-RBNE033 KMA "Composti molecolari e materiali ibridi nanostrutturati con proprietà ottiche risonanti e non risonanti per dispositivi fotonici". T.B. thanks the Dipartimento di Chimica Organica e Industriale of the University of Milan for hospitality. We thank Prof. F. Bonomi and Prof. S. Iametti (DISMA, University of Milan) for assistance and helpful suggestions in CD spectra recording experiments.

[1] "Chiral monodentate phosphorus ligands": C. Bruneau, J. L. Renaud in *Phosphorus Ligands in Asymmetric Catalysis* (Ed.: A. Börner), Wiley-VCH, Weinheim **2008**, pp. 5–35, and references herein.

[2] M. R. Whitnall, K. K. Hii, M. Thornton-Pett, T. P. Kee, *J. Organomet. Chem.* **1997**, *529*, 35; M. T. Powell, A. M. Porte, K. Burgess, M. T. Powell, *Chem. Commun.* **1998**, 2161; A. M. Porte, J. Reibenspies, K. Burgess, *Tetrahedron* **2001**, *57*, 5027; P. Wyatt, H. Eley, J. Charmant, B. J. Daniel, A. Kantacha, *Eur. J. Org. Chem.* **2003**, 4216; F. Sannicolò, T. Benincori, S. Rizzo, *Triarilfosfine chirali a simmetria C_3 come leganti di metalli per la preparazione di catalizzatori per reazioni stereoselettive*, Italian Patent MI2005A 002029; Á. Pintér, G. Haberhauer, I. Hyla-Kryspin, S. Gromme, *Chem. Commun.* **2007**, 3711.

[3] M. Ciclosi, J. Lloret, F. Estevan, P. Lahuerta, M. Sanau′, J. P. Prieto, *Angew. Chem.* **2006**, *118*, 6893; *Angew. Chem. Int. Ed.* **2006**, *45*, 6741.

[4] P. Finocchiaro, D. Gust, K. Mislow, *J. Am. Chem. Soc.* **1973**, *95*, 8172; P. Finocchiaro, D. Gust, K. Mislow, *J. Am. Chem. Soc.* **1974**, *96*, 3198; P. Finocchiaro, D. Gust, K. Mislow, *J. Am. Chem. Soc.* **1974**, *96*, 3205.

[5] W. D. Hounshell, C. A. Johnson, A. Guenzi, F. Cozzi, K. Mislow, *Proc. Natl. Acad. Sci. USA* **1980**, *77*, 6961; F. Cozzi, A. Guenzi, C. A. Johnson, K. Mislow, W. D. Hounshell, J. F. Blount, *J. Am. Chem. Soc.* **1981**, *103*, 957; C. A. Johnson, A. Guenzi, K. Mislow, *J. Am. Chem. Soc.* **1981**, *103*, 6240; C. A. Johnson, A. Guenzi, R. B. Nachbar, Jr., J. F. Blount, O. Wennerström, K. Mislow, *J. Am. Chem. Soc.* **1982**, ***104***, 5163; H.-B. Bürgi, W. D. Hounshell, R. B. Nachbar, Jr., K. Mislow, *J. Am. Chem. Soc.* **1983**, *105*, 1427; A. Guenzi, C. A. Johnson, F. Cozzi, K. Mislow, *J. Am. Chem. Soc.* **1983**, *105*, 1438; H. Iwamura, K. Mislow, *Acc. Chem. Res.* **1988**, *21*, 175.

[6] Y. Kawada, H. Iwamura, *J. Org. Chem.* **1980**, *45*, 2547; Y. Kawada, H. Iwamura, *J. Am. Chem. Soc.* **1981**, *103*, 958; Y. Kawada, H. Iwamura, *Tetrahedron Lett.* **1981**, *22*, 1533; Y. Kawada, H. Iwamura, *J. Am. Chem. Soc.* **1983**, *105*, 1449; Y. Kawada, H. Iwamura, Y. Okamoto, H. Yuki, *Tetrahedron Lett.* **1983**, *24*, 7910; N. Koga, Y. Kawada, H. Iwamura, *J. Am. Chem. Soc.* **1983**, *105*, 5498; Y. Kawada, Y. Okamoto, H. Iwamura *Tetrahedron Lett.* **1983**, *24*, 5359; H. Iwamura, T. Ito, K. Toriumi, Y. Kawada, E. Osawa, T. Fujiyoshi, C. Jaime, *J. Am. Chem. Soc.* **1984**, *106*, 4712; N. Koga, H. Iwamura, *J. Am. Chem. Soc.* **1986**, *108*, 1426; H. Iwamura, *J. Mol. Struct.* **1985**, *126*, 401; N. Koga, Y. Kawada, H. Iwamura *Tetrahedron* **1986**, 42, 1679; Y. Kawada, H. Yamazaki, G. Koga, S. Murata, H. Iwamura, *J. Org. Chem.* **1986**, *51*, 1472; N. Koga, H. Iwamura, *Chem. Lett.* **1986**, 247; Y. Kawada, J. Ishikawa, H. Yamazaki, G. Koga, S. Murata, H. Iwamura, *Tetrahedron Lett.* **1987**, *28*, 445.

[7] K. Mislow, *Acc. Chem. Res.* **1976**, *9*, 26.

[8] R. Glaser, J. F. Blount, K. Mislow, *J. Am. Chem. Soc.* **1980**, *102*, 2777.

[9] The first resolution of the racemate of residual enantiomeric propellers was claimed for some asymmetric tris(aryl)ethylenes; however, this cannot be considered as residual, since these systems are classical atropisomers, exhibiting a stereogenic axis located on the intersection of the plane of the labeled aromatic ring with the plane of the double bond: S. E. Biali, Z. Rappoport, A. Mannschreck, N. Pustet, *Angew. Chem.* **1989**, *101*, 202; *Angew. Chem. Int. Ed. Engl.* **1989**, *28*, 199; E. Rochlin, Z. Rappoport, F. Kastner, N. Pustet, A. Mannschreck, *J. Org. Chem.* **1999**, *64*, 8840.

[10] B. Laleu, G. Bernardinelli, R. Chauvin, J. Lacour, *J. Org. Chem.* **2006**, *71*, 7412.

[11] C. Foces-Foces, F. H. Cano, M. Martinez-Ripoll, R. Faure, C. Roussel, R. M. Claramunt, C. Lopez, D. Sanz, J. Elguero, *Tetrahedron: Asymmetry* **1990**, *1*, 61.

[12] T. Benincori, G. Celentano, T. Pilati, A. Ponti, S. Rizzo, F. Sannicolò, *Angew. Chem.* **2006**, *118*, 6339; *Angew. Chem. Int. Ed.* **2006**, *45*, 6193.,

[13] R. Laser, J. F. Blount, K. Mislow, *J. Am. Chem. Soc.* **1980**, *102*, 2777.

[14] J. Albert, R. Bosque, J. M. Cadena, S. Delgado, J. Granell, G. Muller, J. I. Ordinas, M. F. Bardia, X. Solans, *Chem. Eur. J.* **2002**, *8*, 2279; L. Horner, H. Winkler, A. Rapp, A. Mentrup, H. Hoffmann, P. Beck, *Tetrahedron Lett.* **1961**, *2*, 161; S. Otsuka, A. Nakamura, T. Kano, K. Tani, *J. Am. Chem. Soc.* **1971**, *93*, 4301; W. S. Knowles, M. J. Sabacky, B. D. Vineyard, *J. Chem. Soc. Chem. Commun.* **1972**, 11; K. Tani, L. D. Brown, J. Ahmed, J. A. Ibers, M. Yokota, A. Nakamura, S. Otsuka, *J. Am. Chem. Soc.* **1977**, *99*, 7876; B. Bodganovic, B. Henc, A. Lösler, B. Meister, H. Pauling, G. Wilke, *Angew. Chem.* **1973**, *85*, 1013; *Angew. Chem. Int. Ed. Engl.* **1973**, *12*, 954; T. Yoshikuni, J. C. Bailar Jr. , *Inorg. Chem.* **1982**, *21*, 2129; J. Albert, J. M. Cadena, J. Granell, G. Muller, J. I. Ordinas, D. Panyella, C. Puerta, C. Sañudo, P. Valerga, *Organometallics* **1999**, *18*, 3511; V. V. Dunina, L. G. Kuz′mina, M. Y. Rubina, Y. K. Grishin, Y. Veit, E. I. Kazakova, *Tetrahedron: Asymmetry* **1999**, *10*, 1483; P. Antognazza, T. Benincori, S. Mazzoli, F. Sannicolo, T. Pilati, *Phosphorus, Sulfur Silicon Relat. Elem.* **1999**, *144*, 405; J. Albert, R. Bosque, J. M. Cadena, J. Granell, G. Muller, J. I. Ordinas, *Tetrahedron: Asymmetry* **2000**, *11*, 3335; T. Benincori, E. Cesarotti, O. Piccolo, F. Sannicolò, *J. Org. Chem.* **2000**, *65*, 2043; T. Benincori, R. Cirilli, R. Ferretti; F. La Torre, O. Piccolo, L. Zanitti, *Chromatographia* **2002**, *55*, 25; F. La Torre, O. Piccolo, L. Zanitti, *Chromatographia* **2002**, *55*, 25.

[15] Symbol *a* indicates that the prioritary edge (Cahn–Ingold—Prelog (CIP) rules) of a ring is *anti* to the P–O bond (or to the lone pair) and located below the reference plane (the plane defined by the three carbon atoms connected to the P centre); *s* indicates a *syn* relationship. Alternative descriptors for propellers have been suggested; however, they require the introduction of symbols not familiar to the stereochemical language; R. A. Baber, A. G. Orpen, P. G. Pringle, M. J. Wilkinson, R. L. Wingad, *J. Chem. Soc. Dalton Trans.* **2005**, 659, and reference therein.

[16] J. Tomasi, M. Persico, *Chem. Rev.* **1994**, *94*, 2027.

[17] For instance, one may recall that the rotation barrier in ethane is ≈ 3 kcal mol^{-1}; N. Moazzen-Ahmadi, H. P. Gush, M. Halpern, H. Jagannath, A. Leung, I. Ozier, *J. Chem. Phys.* **1988**, *88*, 563.

[18] P. K. Mandal, E. Arunan, *J. Chem. Phys.* **2001**, *114*, 3880.

[19] D. M. P. Mingos, T. E. Müller, *J. Organomet. Chem.* **1995**, *500*, 251; T. E. Müller, J. C. Green, D. M. P. Mingos, C. M. McPartlin, C. Whittingham, D. J. Williams T. M. Woodroffe, *J. Organomet. Chem.* **1998**, *551*, 313; S. Sasaki, K. Sutoh, F. Murakami, M. Yoshifuji, *J. Am. Chem. Soc.* **2002**, *124*, 14830; S. Sasaki, R. Chowdhury, M. Yoshifuji, *Tetrahedron Lett.* **2004**, *45*, 9193.

[20] K. Naumann, G. Zon, K. Mislow, *J. Am. Chem. Soc.* **1969**, *91*, 7012.

[21] H. A. Bent, *Chem. Rev.* **1961**, *61*, 275; R. D. Baechler, W. B. Farnham, K. Mislow, *J. Am. Chem. Soc.* **1969**, *91*, 5686; R. D. Baechler, K. Mislow, *J. Am. Chem. Soc.* **1970**, *92*, 3290; A. Rauk, L. C. Allen, K. Mislow, *Angew. Chem.* **1970**, *82*, 453; *Angew. Chem. Int. Ed. Engl.* **1970**, *9*, 400; R. D. Baechler, K. Mislow, *J. Am. Chem. Soc.* **1971**, *93*, 773; R. D. Baechler, J. D. Andose, J. Stackhouse, K. Mislow, *J. Am. Chem. Soc.* **1972**, *94*, 8060; E. Magnusson, *Aust. J. Chem.* **1985**, *38*, 23.

Received: October 31, 2008

